THE DISTRIBUTION OF DUST GRAINS OF ALL TEMPERATURES IN NORMAL SPIRAL GALAXIES – TOWARD A UNIFIED OBSERVATIONAL PICTURE

D.L. Block[1], B.G. Elmegreen[2], A. Stockton[3], M. Sauvage[4]
[1] *University of the Witwatersrand, Private Bag 3, WITS 2050, South Africa.*
[2] *IBM Research Division, T.J. Watson Research Center, P.O. Box 218, Yorktown Heights, NY 10598, USA.*

[3] *IFA, University of Hawaii, 2680 Woodlawn Dr. Honolulu, HI 96822, USA.*
[4] *CEA/Service d´ Astrophysique, C.E. Saclay, F-91191 Gif-sur-Yvette, France.*

Abstract

Through their extinction variations at arcsecond resolution in $B-K$ and other broad-band color images, large $0.1\mu m$ dust grains provide an unparalleled high-resolution tracer for gas dynamical processes. Cold (15K-25K) dust traces the molecular component of the interstellar medium, and through it, the precursors to star formation; it delineates shocks in the form of thin shells or dust lanes; it reveals large-scale gaseous processes that are not present in the stars, and vice-versa, and it signals the presence of far-reaching nuclear winds or radiative processes that send gas to great heights off the disk, where interstellar matter was not formerly thought to exist. Cold dust is the most sensitive high resolution tracer of interstellar gas dynamics that is available: in many galaxies, the average optical depth is conveniently equal to unity at visual wavelengths, which means that gas compressions that are even only a factor of 2 can turn a region from bright to dark, permitting groundbased observations at sub-arcsecond resolution. Such compressions include most interstellar gas processes, leading to cold dust images that are finely interwoven with filaments, clouds, shells and other evidence for complex gas behavior. NGC 4736 provides an example of this structure in a galaxy that is optically dominated by long spiral arms. NGC 2841 offers an example of the opposite extreme: long, smooth and regular dust arms in a galaxy that is optically extremely patchy and flocculent.

Next, we present, for the first time, a *unified* view of dust grains of all sizes in a galaxy. We combine optical with mid-infrared ISOCAM images of the Whirlpool spiral galaxy M51 and its companion NGC 5195. The image reveals remarkable interarm *spirals* of dust and hot skins around dense cold clouds. A ring of dust surrounds the nucleus of NGC 5195.

1 Introduction

Fundamental to extragalactic astronomy is the classification of spiral galaxies. What has only now been truly brought to the fore is just how inextricably intertwined and dependent galaxy morphology is upon the extinction caused by dust grains.

The tracing of dust grains in nature can be very elusive: firstly, optical depths inferred from dust *attenuation* effects – observed reductions in the surface brightness profiles of dusty galaxies – can be quite misleading, because scattering by dust grains may fill in at least part of the lost surface brightness; the true *extinction* = absorption+scattering optical depths can be much larger.

Secondly, while the infra-red universe had been spectacularly revealed by the Infrared Astronomy Satellite IRAS, Mayo Greenberg had predicted that the large (tenth micron) dust grains *responsible* for the actual visual extinction in dusty galaxies would have temperatures of only $\sim$ 16 K in the diffuse medium (eg. [43], [46]): far too cold to be detected in external galaxies by IRAS. Could it be that astronomers had underestimated galaxy dust masses by up nearly one order of magnitude [17] and that IRAS observations were only sensitive to the smaller, hundredth micron dust population?

Sub-mm/mm observations of spiral galaxies had brought the issue of cold dust to the fore, but with controversial and diametrically opposed conclusions (eg. compare [33] and [34]). For the large grains, an *evolutionary* model consisting of silicate core-organic refractory and ice mantle grains was considered appropriate by Greenberg as early as 1973 (see [44]; also Désert et al. [28]). Quantitative techniques to probe the full spatial extent of dust grains of all temperatures, at arcsecond resolution, are clearly called for.

In this *Moriond97* discourse, we wish to elucidate a number of key points:

2 What is the upper limit in the size distribution of a dust grain?

While an upper limit cut-off of 0.25 μm is usually adopted for the radii of the largest dust grains in the diffuse ISM, we should remember that, at present, we do *not* know the definitive answer to the above question. Optical and near-infrared dust albedos *may be identical*, as first proved by Witt and his collaborators [102] for the NGC 4826 dust screen, and more recently by Block [19], for dust grains in that spiral arm of M51 which lies juxtaposed in front of the companion NGC 5195. The possibility of near infrared *emission* may be partly responsible for the very high albedo at K or K', and this needs to be carefully evaluated. However, results on both the theoretical (e.g. Kim, Martin and Hendry [57]) and observational (eg. Lehtinen and Mattila [63]) fronts suggest that large dust grains may be at least 0.5 μm in radii – *twice as large* as attested to from standard silicate-graphite dust models [30].

On the basis of the standard models, most interstellar grains were thought to be substantially smaller than near-infrared wavelengths. One would *a priori* have expected that the near-infrared albedo to be $\sim$ 0.2, i.e., reduced by a factor of 3 compared to the optical V albedo of 0.6. As noted above, the expectations now are that $a(K) \sim 0.6$ and $a(V)$=0.6, i.e., the ISM may contain large grains whose optical and near-infrared albedos may be identical.

Remark: Scattering in the near-infrared is highly important [102], [19]. In Block, Elmegreen and Wainscoat [18], we have proposed that scattering by large dust grains may be responsible for the pronounced asymmetry found in the colour gradient of inclined systems such as NGC2841, especially the *washing out* and bluing of the far-side of such a disc (see also section 6).

3 Lessons from IRAS, ISO & the Submm

The inversion of a spectral energy distribution (SED) into a dust *temperature* distribution is a poorly conditioned problem. As demonstrated by Hobson and Padman, markedly *different* dust temperature distributions can be secured from an *identical set* of 30–1300 μm flux measurements [53].

The dilemma concerning the detection of (cold) dust in extragalactic systems and the determination of its mass may be summarised as follows:

3.1 Cold Dust: IRAS, ISO and the Submm

Cold (15–25 K) dust is not seen by IRAS (see Figure 8 in Sauvage and Thuan [88]). The far-IR emission spectrum from interstellar dust is much broader than a Planck curve for a single temperature. While the IRAS bands at 12, 25, 60 and 100 μm are able to delineate the emission from very small, hot grains and warm grains, the peak of the emission spectrum lies *beyond* 100 μm, not detectable by IRAS. Since the scaling of the total infrared emissive power is $\sim T^6$ where T is the grain temperature (Andriesse [5]), cold grains do not emit much energy and add only a small contribution to the low-frequency end of the emission spectrum, even though these cold grains may constitute by far the bulk of the proportion of the dust mass. IRAS dust masses are usually derived from the measured fluxes at 60 and 100 μm and are not sensitive to the flux at longer wavelengths, where the cold dust would radiate.

Using filters from λ= 16 μm to λ = 200 μm on-board the Infrared Space Observatory ISO [56], Rodriguez Espinosa et al. [80] attempted to fit *bimodal dust emission* in three galaxies, but their fitting of the warm and cold dust curves critically depends on values assumed for the dust emissivity index, as highlighted below.

3.2 Sensitivity in β variations

Apart from the SED inversion problem being poorly conditioned, there are other important reasons why sub-mm observations are far from ideal for determining even the amount of dust which *is detectable* at those wavelengths. Chini and Krügel [26] highlight the fact that the wavelength dependence of the dust absorption efficiency in the far-IR and sub-mm region is poorly known (Hildebrand [50], Clements *et al.* [27]). Kwan and Xie [61] conclude that the biggest uncertainty in the determination of dust masses is associated with the uncertain dust emissivity law. As elucidated further by Gordon [41], a change of only 20% from β=2 (i.e., β = 1.6 or 2.4) will cause a 50% error in the ratios of optical depths at 400 and 1300 μm.

3.3 Very cold dust not seen even in the sub-mm

Very cold dust (< 15 K) will not be seen *even* at sub-mm to mm wavelengths, as beautifully demonstrated by Pajot *et al.* [72]. In some instances such nondetection has led to claims that very cold dust is simply not present (Clements *et al.* [27]; Carico *et al.* [24]; Eales, Wynn-Williams, and Duncan [34]; Stark *et al.* [95]). What are lower temperature limits for a dust grain? In a remarkable presentation at a recent International Dust-Morphology Conference, Duley [31] convincingly argued that grain temperatures can actually fall below 2.7 K – the temperature of the cosmic microwave background – in the case of very small grains subject to temperature spiking.

Of course, the largest mass fraction of interstellar dust resides in the biggest grains, often found in the densest and coldest environments where accretion and coagulation may be

important and where radiative heating is weak (Figure 4 in Greenberg and Li [46] is most instructive).

3.4 Beam sizes and Side-lobes: Submm studies

3.4.1 Submm Telescopes: Beam size considerations Observations at different wavelengths with different beam sizes are difficult to compare. Modern sub-mm telescopes have beam sizes of order 20″ or less, and they are often joined with IRAS data obtained at $\sim$ 120″ resolution. The uncertainty in the estimate of the average far-infrared (FIR) to mm flux ratio amounts to one order of magnitude (or more). We look forward to hearing at this *Moriond97* Conference of the combination of recent SCUBA and ISO data in this regard.

Remark: When evaluating far-IR/submm ratios, it is imperative that the entire galaxy be observed – and not just the central (bulge) area – as cold dust can be very widespread – see section 4.

3.4.2 Submm Telescopes: Extended SideLobes The 'error beam' (extended side lobes) of sub-mm/mm telescopes operating near their minimum working wavelength can be very important, resulting in large calibration uncertainties and difficulties in comparing point and extended sources (J. Lequeux and C. Purton: private communications).

3.5 Dust masses and H_2 column densities

The inference of dust masses from CO observations relies on a *very* uncertain derivation of H_2 column density from the CO line intensities (see especially section 4.3 in Allen and Lequeux [2] and section 3 in Lequeux, Allen and Guilloteau [64]). Here ISO promises spectacular results, with the first direct extragalactic detection by Valentijn et al. [98] of the pure rotational H_2 S(0) and S(1) lines in the galaxy NGC 6946. It is becoming clear that a CO/H_2 conversion determined for galactic GMCs can overestimate the true H_2 mass in some cases (e.g., the ISO observations of NGC 6946, Valentijn *loc.cit.*) while in other galaxies, a standard 'Galactic' conversion can underestimate the H_2 mass (see the beautiful description by Allen [3]).

3.6 Dust-gas ratios

Furthermore, dust-to-gas ratios themselves still need to be confirmed. A full discussion of this problem for the SMC is presented by Lequeux [65]. It is well known that dust-to-gas mass ratios in spiral galaxies observed by IRAS are exceptionally low [88], by $\sim$ an order of magnitude, compared to the standard value in our Galaxy. The mean [warm dust]-to-gas mass ratio determined by Devereux and Young [32] for 58 spirals is $\sim$ 1/1080 (with a similar conclusion reached by Sanders, Scoville and Soifer [87]), compared to the canonical Galactic value of $\sim$ 1/150.

4 A new perspective on cold dust from optical/NIR imaging

At alternative approach is to study the distribution of dust grains of all temperatures from optical/NIR imaging, combining these with radiative transfer models invoking both absorption and multiple scattering to estimate dust masses [16], [17]. The extinction cross section of a dust grain is independent of its temperature. With the coming-of-age of modern NIR camera arrays, the spatial distribution of tenth micron dust grains of all temperatures can be studied at

unprecedented arcsecond resolution[16], [19]: two orders of magnitude better than attainable by IRAS and one order of magnitude better than presently attainable with the largest sub-mm/mm telescopes.

Colour probes such as $V-K$ (or $V-K'$) are almost totally dominated by the extinction at V, allowing V optical depths to be properly and correctly evaluated.

4.1 Widespread, Optically Thin Interarm Dust in NGC4736 and NGC 2997

The pattern in the distribution of the interarm dust we see in NGC 4736 (colour plate 4 in Block [19]) is reminiscent of the distribution of discrete dust clouds in M31 (which do not appear to show any affinity to the spiral structure of M31) mapped by Hodge [54]. On the basis of observed B and K' surface brightness profiles and the $B-K'$ colour map – which includes the entire H II ring from −50 to +50 arcsec – we conclude that the dust is *embedded* rather than contained in an overlying, foreground screen. This conclusion is based on the widespread presence of filamentary structures in $B-K'$ colour cuts (eg. Figure 2 in [16]), the ratio of visual extinctions to colour excesses, and the relatively large 0.33 ratio of L(IR)/L(Opt) (a factor two higher than that for the NGC 4826 screen geometry).

Typical reddening values are $E(B-K') = 0.2$ or more in the interarm regions [increasing to 0.6 – 0.8 in the actual dust spirals themselves, where values for $B-K'$in the dust lane 20″ NW from centre attain 4 magnitudes].

That the cold interarm dust is illuminated by the old stellar Population is in excellent accord with Figure 2 and Figure 5 of Smith [94] and Smith et al. [93] respectively. She finds that the distribution of the 100 μm emission does *not* trace the spatial distribution of young stars delineated from Hα+[N II] observations but *does* trace the distribution of old stars seen through their broadband red (F) image.

For a 'dusty galaxy' model (see Witt, Thronson and Capuano [101]; hereafter WTC), this colour excess corresponds to V optical depth values in the interarm regions, of order 0.75. [In the optically thick dust lanes of NGC 4736, the inferred optical depths in V, for the same 'dusty galaxy' WTC model, imply values $\tau(V)$ in the range of 2–4 [16]. The *average* V optical depth through the disk is of order unity.]

Adopting a distance to NGC 4736 of 7 Mpc (Sandage and Tammann [85] with $H_0 = 50$ km s^{-1} Mpc^{-1}) and integrating over the inner disk out to a radius of 60 arcseconds, yields a dust mass of $3 \times 10^6 M_\odot$. If the 'cloudy' dust model of WTC is used – where there is a filling factor of 0.33 – the dust mass approaches $6 \times 10^6 M_\odot$. For the radiative transfer in a multiphase, clumpy medium in NGC 4736, all dust estimates will be even *larger* (Hobson and Scheuer [51]; Hobson and Padman [52]). By contrast, the dust mass of NGC 4736 derived from IRAS data is only $7 \times 10^5 M_\odot$ (See Figure 7*b* of Sage [82]). This clearly illustrates that the bulk of the dust mass is apparently at low enough temperatures to have been undetected by IRAS and that the IRAS dust mass underestimates the total dust mass by $\sim$ 900%. Furthermore, the Galactic dust-gas ratio then becomes representative of that for NGC 4736.

Lesson 1 from Optical/NIR imaging: The actual colour excess E($B-K$) and derived optical depth τ(V) of the interarm dust may be *small.* However, because the spatial distribution of the [cold] interarm dust may be so *widespread*, the cold dust mass, when integrated over the galactic disk, can represent 90% of the total dust mass – as it does for NGC 4736.

For the very widespread interarm dust in NGC 2997, covering several minutes of arc, the reader is referred to our $B-K'$ colour map of that galaxy (see Fig. 6 in ref. [16]).

Lesson 2 from Optical/NIR imaging: ISO or submm observations of only the *central region* of a galaxy such as NGC 2997 may detect the warm/hot dust surrounding the hot-spot nucleus, and may lead to the conclusion that only warm dust is present. True, but only

applicable to the central area observed. Certainly, the very central regions of galaxies are not where we would expect to find widely distributed, optically thin [cold] interarm dust we see in our optical/NIR images.

If submm/mm experiments, for example, were to cover the *entire extent* of the galaxy, such as the 1-2mm study by Andreani and Franceschini [4] of the Magellanic Clouds, a substantial millimetric emission, implying the existence of large amounts of cold dust, could indeed be found.

4.2 Long Dust Spirals in the Optically Flocculent Prototype NGC2841

Over 60% of isolated, non-barred galaxies have a flocculent, 'fleece-like' appearance. A characteristic of such galaxies is that the optical patches, by definition, span only a small range in azimuth. Optical images of flocculent galaxies show no grand design spiral structure in the underlying stellar disk ([84], [35], [58], [103]).

One of the prototypes of a flocculent galaxy is NGC 2841. In collaboration with Bruce Elmegreen and Richard Wainscoat, we have imaged and studied this galaxy in the near-infrared (see [18]).

NGC 2841 has a typically large bulge for its Hubble type S(r)b, and a very high rotation rate, 270 km s^{-1}, in most of the disk beyond the bulge where the gas is concentrated in a ring with peak surface mass density $\sim 21 M_{\odot}$ pc^{-2} ([20], [7], [106], [22]).

No bright stellar waves are seen in our K' image of NGC 2841 ([18], [19]). Usually such waves are obvious at K' ([14], [15], [77]). In their pioneering study of azimuthal Fourier decompositions of K'-band light, Rix and Zaritsky [78] showed the arm/interarm contrasts for most spiral arms are a factor 2 or more. The lack of bright K' spirals in NGC 2841 implies that any stellar waves that may be present are weaker than in grand design spirals by at least a factor of ten.

What is clear in our first K' image of NGC 2841 (see Fig 1*b* in [18]) are the remarkable two long and regular *dark* spirals (one outer, one inner) extending from the northeast minor axis to the north, and the other set of dark spirals in the west and south. The dust+gas spirals are seen even more clearly when we illuminate the N–NE section of the disk (Fig 1*c* in [18]). The dark K' spiral closest to the bulge in the northeast contains a most unusual amorphous strip of emission in the optical photograph, arrowed in Fig. 1*a* of Block, Elmegreen and Wainscoat [18].

A deprojected and enhanced image from our combined V and K' data appears on page 640 of [19]. The deprojection was made by assuming a position angle of 150° and an inclination of 68°. Tightly wound arms span azimuthal angles of around 160°. The K′ band extinctions through the inclined disk viewed with 68° inclination are equal to 1.32 mag and 0.68 mag respectively [18] at the locale of the inner and outer dark spirals; the corresponding extinction at V is therefore 13.2 mag and 6.8 mag respectively.

The rotation of NGC 2841 is receding on the southern major axis (Bosma [20]), so the near side of the galaxy is the northeast minor axis if all the spirals are trailing. This means that the bright diffuse V-band patch in the inner dark NE K'-band spiral is on the near side of the galaxy, in front of the bright bulge. There are no other bright diffuse patches of similar extent in this galaxy and this one is exactly on the minor axis. This position suggests that the diffuse optical emission is from bulge light scattered off the top of the gas+dust spiral seen in K' (see also section 6). We *predict* that the spectrum of this diffuse patch should contain stellar absorption lines similar to those in the bulge stars.

5 Spiral density waves (SDWs) are not always required to organise dust into coherent dust lanes

5.1 The Western Spiral Arm in NGC 2997

Optically, the grand design ScI spiral galaxy NGC 2997 (eg. Marcelin et al. [68]) possesses two dominant spiral arms, one northern, one southern. The reader is referred to the IIIaJ+GG385 blue-band photograph published as Fig. 2*a* in ref. [15], where the arms are labelled B–C and D–E respectively. The southern arm has a prominent western branching into a third arm (segment E–F in that photograph). In Fig. 2*a* in [15], star formation in the western spiral arm segment E–F is apparently just as conspicuous as it is in the northern and southern spiral arms.

Striking, however, is the virtual absence, in the near-infrared, of the western branching E–F so prominent optically. *A stellar density wave is apparently not responsible for for organizing the long coherent dust lanes along the western spiral arm of NGC 2997.* That arm sector must be primarily gaseous.

These findings are in excellent accord with the study by Elmegreen and Elmegreen [36] that the star formation rate per unit gas mass in a galaxy is totally independent of whether the galaxy has spiral density waves (SDWs) or not: in the western arm of NGC 2997, star formation in that sector has clearly proceeded independently of a density wave there.

That SDWs must be present to *trigger* star formation is not true. Different processes in the same galaxy may be responsible for the formation of stars. SDWs can be effective in collecting most of the gas along the waves: in an Hα study of NGC 2997, Milliard and Marcelin [67] found that the southern arm (D-E) showed more compact and brilliant HII regions compared to the northern arm (see their Figure 5). Now NGC 2997 reveals a distinct $m = 1$ asymmetry in its stellar Population II disk. The southern arm D–E is definitely more pronounced than the northern arm B–C at 2.1 μm, while the northern interarm region is significantly brighter than its southern counterpart. Indeed, a Fourier analysis shows that the $m = 1$ amplitude is about 50% that of the $m = 2$ component. The most natural interpretation is that there are two dominant modes, $m = 1$ and $m = 2$, with negative interference on the northern side. Clearly, the conclusion of Elmegreen and Elmegreen [36] is again affirmed: SDWs can be very effective in the organization of gas along waves but they are not a prerequisite for star formation – as we see for the western gaseous segment in the same galaxy.

5.2 Coherent Dust spirals Organized by Shear?

That "long, coherent dust spirals are always associated with classic optical star formation tracers [OB stars, H II regions]" is not always true: Black NIR dust + gas spirals *with no associated star formation in the arms* have been identified.

An intriguing possibility is that the dark IR spirals in NGC 2841 may be the result of shear [19]. Large, cold clouds with no obvious signs of associated star formation (such as G216-2.5 in our Galaxy [69], [100]) may simply have been subjected to the enormous shear in NGC 2841 of 54 km s^{-1} kpc^{-1}. The column densities at the locale of the dark IR spirals are reminiscent of those for the Rosette GMC. Of course the Rosette GMC extends for only 3.5 degrees (see Blitz and Thaddeus [12] and Block [13] for morphological descriptions). Our dark dust+ gas spirals, spanning 160° in azimuth, *may* be a collection of high mass clouds which have been subjected to very large rates of shear.

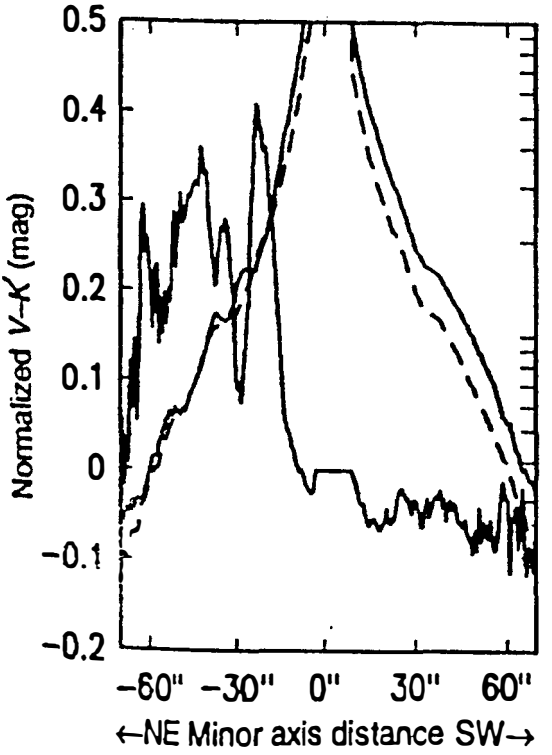

Figure 1: Minor axis V and K′ profiles (centrally peaked curves) and V-K′ relative magnitude difference for NGC 2841. The minor axis on the *far* side of the galaxy (positive distance offset in the figure) is the *bluest.* There is a strong red-blue gradient from the near (NE) to the far-side (SW) minor axis, which we attribute [18] to scattering by dust grains at high z.

6 A Halo of dust grains at high z

Dust grains may be located at high galactocentric latitudes, possibly forming a halo – a few kpc in radial z direction – above the bulge and plane of the disk. Scattering by dust grains at high z distances into our line of sight can then lead to pronounced $V-K$ or $B-K$ colour gradients (red to blue, from near to far-side) for well-inclined systems. That the dust lanes on one side of the bulge often appear more prominent on the near-side than those on the far side (eg. Lynds [66], Sandage [84]) may indeed betray the presence of a halo of dust grains surrounding the entire galaxy, rather than forcing a foreground dust sheet or screen.

The red to blue colour gradient in NGC 2841 (see Figure 1) can be explained by scattered light from dust located high off the plane in the region of the bulge. In such a position, dust will selectively scatter blue bulge light at high angles into our line of sight and leave the direct paths redder; this makes the bulge and far-side *bluer* and more uniform than the near side.

The fact that the blue excess occurs at a projected distance from the galaxy center $\sim$ 3 kpc

(lower limit) implies that a substantial amount of dust has to be outside the deep potential well of the bulge. Radiation pressure and a nuclear wind may be involved. The colour gradient with distance is faintly evident in the Wray Colour Atlas [105] where the bulge and far-side minor axis look white and washed out compared to the near-side minor axis. (The effect is much stronger in our data because the wavelength range covered by our V and K' bands is larger).

Inspection of many Atlas photographs shows this asymmetry in a whitening/washing out of resolution on the far side, which we suggest may be attributed to scattering of dust grains at high z into our line of sight [18]. As noted in a comment by Phil James at Les Arcs, one clearly sees such an asymmetry even for our closest spiral neighbour, M31.

Thornley [97] has secured optical and near-infrared images of NGC 5055, another prototypical flocculent. She comments that *'the distribution of extinction in NGC 5055 is very asymmetric: optical depths in the northern half of the galaxy are approximately 0.5, increasing to 4-5 against the southern half of the galaxy'*. In a question to Thornley, she advised us (private communication) that the very reddened side was the near-side; the distinctly bluer side was the far-side; exactly the same scenario as for NGC 2841.

In conclusion, Grosbøl and Patsis [47] noted that the galaxies NGC 3223 and NGC 5085 showed a significant $V-K'$colour gradient along a direction perpendicular to their major axis. We predict that it will be the far-side that will be found to be bluer and that it will be the near-side that will be found to be redder.

Remark: Screen geometries need not be invoked to explain red to blue colour gradients from the near to far side of a galaxy. Such a gradient may simply betray a halo of dust grains at high z – high off the plane – around the entire galaxy, prefentially forward scattering (blue) light into our line of sight. The presence of a halo of cold dust at high z could herald the presence of a halo of very cold [molecular hydrogen] gas which may be an important constituent of dark matter (Pfenniger and Combes [73]).

The bright amorphous strip of optical emission in the $\tau(V) \sim 13$ dust lane on the near (NE) side of NGC 2841 finds a natural explanation, too, in terms of scattering of bulge light by dust grains at high z [18] – bulge light being scattered off the top of the dense gas+dust spiral seen in K', with the mid-plane stars obscured.

Do we have evidence that bulges themselves can be dusty? This is our next point of focus in this review.

7 Dust in bulges and discs

In several papers, the words *dusty disks* have been used to imply optically thick discs. We hope that we have dispelled that notion: a dusty disk need not necessarily be optically thick everywhere with $\tau(V)>> 1$; it may be optically thin in the interarm areas, but containing widespread interarm dust there; when the integrated dust mass over the galactic disc is computed, this may be an order of magnitude higher than the [warm] IRAS dust mass.

Not only can discs be dusty, but bulges can, too. In fact, dust lanes may extend right in toward the nucleus of some galaxies. For example, HST imaging of the nuclear regions of the Andromeda Galaxy M31, and of M33, shows that these two Local Group spirals have considerable dust complexes in the inner 100 parsecs of their nuclei (see Rich et al. [76], and earlier groundbased studies by Johnson and Hanna [55] and by McElroy [71]).

Our optical/nearIR imaging of NGC 2997 reveals dust lanes extending right into the nuclear area. This is also true of the dust lanes extending within the nuclear region of NGC 4736 (see the magnificent unsharp masked photograph in Kormendy [59]).

There may be much more continuity between bulge and disc (in dust content, metallicity, age and kinematics) than first thought when bulge/disk decompositions were proposed, as has already been alluded to by Rich and by other investigators; for excellent reviews, see Kormendy [59], [60].

With an inhomogeneous dust distribution extending so close to the nuclei of certain galaxies, it would be natural to sometimes expect an asymmetry in the central light and colour distribution, and for the nucleus itself to be optically offset in some instances – the result of an optical depth effect. This is our next item of discussion.

8 Central Dust and Off-centered nuclei

Two examples are noted here (NGC 4736 and NGC 5195) where there is an asymmetry in the central light distribution: while K' surface brightness profiles are symmetric about the stellar mass centroid, B or V surface brightness profiles may show an asymmetric shift from the centre– in other words, optical depth effects caused by central dust extinction may lead to apparently off-centered nuclei.

For NGC4736, the reader is referred to Figure 8 in ref. [15], where a 4-m Mayall reflector plate of the galaxy (secured by Dr A. A. Hoag) intentionally contains two images on the same plate.

In that Figure, we have superimposed (i) a short (one minute) exposure showing the galaxy centre, printed in positive (white) format, on (ii) a longer (ten minute) exposure, showing the inner spiral arms, printed in negative format. The galaxy centre (white) appears to be misplaced from the geometric centre of the dust distribution in the bulge. In the context of optically thick dusty central regions, this optical offset bears attention: a Fourier analysis *confirms* a m=1 asymmetry in the optical B CCD image. It is interesting to note that the maximum of the molecular CO emission reported by Gérin *et al.* [40] also does not occur at the optical centre (see their Fig. 1*b*), but at a small (10″) offset. The asymmetry of the central light (and colour) distribution is real – the result of an optical depth effect. In our $B-K'$ colour profile [see Figure 2 in [16]], one notes that the region 5″ NW of centre has a far higher optical depth than the adjacent region 5″ of centre to the SE. As discussed in [15] [16], the offset of the small central bar (or oval distortion) no longer manifests itself in the K' optically thin regime – the $m = 1$ Fourier component disappears at 2.1 μm.

The offset of the central light distribution for NGC5195 is likewise apparent when optical and near-infrared surface brightness profiles are compared in their inner regions.

9 A dusty, gaseous Population I disk can cause a grand design stellar Population II disk to masquarade in the optical as a morphologically flocculent specimen

Gaseous and stellar disks can actually fully decouple, so that it is possible for two completely different morphologies to co-exist within the same galaxy. The reader is referred to excellent discussions by Bertin [11] and earlier references [9], [10].

NGC 3223 is a magnificent optically flocculent specimen of Hubble type Sb and van den Bergh speciation I–II. (For an optical photograph, the reader is referred to Panel S4 in Sandage and Bedke [86]). In the near-infrared, however, this galaxy shows bright, grand design SDWs at K' (see Grosbøl & Patsis [47]). If, in the midst of SDWs, SDW pressures are less than the average turbulent gas pressure, the competition between stars and gas is won by gas: the galaxy

would present an *optically* fragmented, flocculent appearance. The star formation history, principally triggered from previous bursts of star formation (rather than SDW pressures), would be stochastic/random. High total gas column densities (and therefore relatively large optical depths at B or V) would be predicted. Indeed, the V optical depth at the radius of the inner ring is ~ 2. The computed dust mass for NGC 3223, assuming a 'dusty' WTC geometry model is 6.4×10^7 $M_\odot$. This is consistent with IR emission described by a Kirchoff-Planck function $B_\lambda(T)$ peaking at a temperature of only T $\sim$ 17 K.

Other optically flocculent galaxies where bright, symmetric two-arm stellar structure in the Population II disk are hidden by dusty Population I disks include NGC 5055 [the stellar arms there span 150° in azimuth]; NGC 2403, NGC 3521 and NGC 4414. Full details are contained in Thornley [96], [97].

10 Concluding Thoughts: A unified view of the spatial distribution of dust grains... New perspectives from the Optical/MIR

10.1 Tracing the distribution of both very small dust grains/PAHS and of large, tenth micron dust grains

In this review, we have demonstrated that colour maps such as $B-K$ or $V-K$ provide a powerful handle to trace the distribution of large, cold tenth micron grains.

It is these large grains which are responsible for the extinction at B or V, and even at K (of course the extinction at K is only 1/10 that at V, but large grains are nevertheless responsible for the extinction at 2 microns).

Now an important constituent of the interstellar medium are tiny grains and polycyclic aromatic hydrocarbons - PAHs (e.g., Sellgren [91] and references therein; Désert, Boulanger and Puget [28]). The Infrared Astronomical Satellite (IRAS) had demonstrated the ubiquity and importance of these tiny grains, which Léger and Puget [62] associated with emission bands at 3.3, 6.2, 7.7, 8.6 and 11.3 μm. Tiny particles are intermediate in size between molecules and classical interstellar grains; characteristic radii are $\sim$ 10 angstroms and $\sim$ 100 atoms per particle [91].

Almost 30 years ago, Greenberg [42] suggested that very small grains could be subject to 'temperature fluctuations'. Studies of the temperature spiking of the very small, hundredth micron particles in response to absorption by photons from the interstellar radiation field (ISRF) have been the subject of intensive investigation (e.g., Duley [31] and references therein).

The temperature spike associated with absorption of a 10eV photon may approach 10^3K [29]. But the timescale for cooling of a very small grain after the absorption of an energetic photon may typically only be about 1 second [31].

If temperature spiking in very small grains is responsible for emission at 15 microns (Sellgren et al. [90]), one could argue that high temperature transients due to stochastic heating in the ISRF will be followed by the grains spending the majority of their time (10^5s - 10^6s) at very low temperatures [these may even be below 2.7 K (Duley [31])].

[An interesting aside for the large dust grains: Greenberg and Li [46] have demonstrated that large grains typically have temperatures of $\sim$ 16 K in the diffuse ISM to $\sim$ 6.5 K at the centre of a molecular cloud (Figure 4 in Greenberg and Li [46]). Tenth micron grains are essentially *always* cold [45]. In that paper, Greenberg computed that a large 0.1 micron dust grain would need to be placed at a remarkably short distance of only 1/10 pc from the intense radiation of an O5 star before the ice would evaporate. He noted [45] that *"silicate cores or bare*

silicate particles or any other refractory particles would be, to all intents, entirely unaffected by evaporation"].

Toward a unified view of viewing dust grains of all sizes, we must include the tiny [hundredth micron and smaller] grains and the PAHs. But the contribution to the *extinction* by these very small grains/PAHs at K or even at B is essentially zero (see Figure 3 of Greenberg and Li [46]). Therefore, $B-K$ or $V-K$ maps show the distribution of large grains *only.*

Let us, however, consider what happens if, instead of subtracting a K image from an optical one, we consider a $B-15$-micron colour map. There is no contribution to the B extinction by very small grains/PAHs, but at 15 μm, there is emission (or equivalently, negative extinction) by these tiny grains/PAHs. In fact, the PAH emission reaches a maximum at approximately 15 microns (see Fig 6 in Greenberg and Li [46]).

Therefore, in a $B-15\mu$m colour map, very small grains *emitting* radiation at 15 microns will show up as areas of apparently enhanced extinction ie. $B-(-15\mu\text{m})$. The 15 μm PAH emission acts, in effect, as negative extinction.

$B-15\mu$m maps are the best probes yet for studying the full range and spatial extent of (1) dust lanes, containing both large tenth micron grains and very small dust grains/PAHs and (2) the diffuse interstellar medium, also containing both large and very small grains. Of course only 12 days (10^6s) before a population of tiny grains is seen in emission, about 1/3 of that tiny grain/PAH population could have been at temperatures of 10K – or even colder (Greenberg and Li, private communication).

Such a $B-15\mu$m image has now been produced for M51 and its companion, NGC 5195 (see Figure 2). The 15 μm mid-infrared image was secured by Sauvage et al. [89] using ISOCAM, the camera on-board on-board the Infrared Space Observatory, ISO (Kessler [56]). For $\lambda =$ 12–17 μm, the filter selected by Sauvage and his collaborators [89] was LW3 (Cesarsky et al. [25]). The groundbased B CCD image was secured at Kitt Peak by T. Boroson.

The relative image scales and orientations were determined by measuring the positions of the nuclei of M51 and NGC 5195 in the two images. The ISOCAM 15 μm LW3 image was rebinned to the B image scale and then rotated and aligned so that the galaxy nuclei in the two images were coincident. The point spread function was determined from stars in the B and from ISOCAM calibration observation. The B image was convolved with the ISOCAM point-spread function, and the LW3 image was convolved with the B point-spread function, resulting in two images of identical angular resolution (7″). Then the ratio of the two images was obtained.

Even at 7″ resolution, the structure in the dust lanes (arm/interarm) and in the diffuse interstellar medium of M51 is striking. While the morphology of the two short inner dust lanes are continuous and extremely regular, spurs and 'bubbles of dust' are beautifully displayed in the outer northern arm. Interarm dust (and presumably any atomic or molecular gas associated with the dust) is unevenly distributed throughout the disk *in the form of spirals.*

The multifrequency photometry observations of Smith [92] 'gives $\sim$ 20 K for the dust temperature observed throughout the main far-infrared features of M51 ... much of this cold dust is probably mixed with a very uneven distribution of molecular and atomic complexes participating in a galaxy-wide episode of star formation'.

There is a remarkable spatial correlation between the extinction from cold dust grains in the B image and the emission from macromolecules/PAHs/small dust grains detected in the ISOCAM image. The interpretation here is that many of the dense cold clouds are surrounded by hot UV-exposed skins.

For its class, the companion NGC 5195 is rather extreme in its starforming properties. Heckman [49] found it to be a member of the LINER class, and 8–13 μm spectral signatures typical of enhanced nuclear star formation were published by Roche and Aitken [79]. Sage

Figure 2: A *unified* view of dust grains of all sizes may be traced in this $B-15\mu$m map of M51 and its companion NGC 5195. Dust grains are coded to appear gray and black. Interarm dust (shaded gray) is distributed *in the form of spirals* in the disk of M51 and a ring of dust surrounds the nucleus of NGC 5195. There is a remarkably close juxtaposition of hot and cold dust, proving the existence of hot skins around dense cold clouds.

and Wrobel [83] found NGC 5195 to have the highest CO luminosity of all the high, L(FIR) S0 galaxies they studied with the NRAO 12-m antenna. van der Hulst et al. [99] report the existence of a rather compact radio source at the nucleus. Smith [92] found an unusually warm dust temperature of 65 K but also noted that *'NGC 5195 has by far the scarcest interstellar medium, amounting to the mass of Sgr B2, a single giant molecular cloud located near the nucleus of the Galaxy.'* NGC5195 has a D_{25} diameter of 5.37′, equivalent to 13.5 kpc at a distance of 8.7 Mpc (Aaronson and Mould [1]).

In this context, it is of great interest to note that the nucleus of the companion galaxy NGC5195 is actually surrounded by a ring of dust. The ring has a radius of $\sim 12''$. Assuming a distance of 8.7 Mpc, $1'' = 42$ pc, the radius of the ring is $\sim$ 500 pc; at a de Vaucouleurs distance of 4.6 Mpc, $1'' = 22$ pc so that the radius of the ring would then be $\sim$ 270 pc.

Boulade et al. [21] had earlier suggested dust enshrouding an active nucleus as a possibility for the generation of the infrared emission of NGC 5195. From our $B-15\mu$m map, the reality of a dusty ring around the nucleus of NGC 5195 is now confirmed.

One is indeed reminded of the obscuring tori of material surrounding other active galactic nuclei (cf. Antonucci [6]).

Remark: A unified view Combining some of the spectacular ISOCAM images with groundbased B or V images allows us, for the first time, to trace the distribution of *both* large grains [responsible for the extinction at B] *and* very small grains [dominating the mid-infrared emission of a normal spiral galaxy] in one single map.

Acknowledgements. DLB is most grateful to G. Mamon, T. Thuan and the Scientific Organizing Committee of the Moriond97 Meeting for their invitation to deliver this review presentation at Les Arcs, Savoie. The research of DLB is supported in South Africa by the Anglo-American and de Beers Chairman's Fund Educational Trust and the University of the Witwatersrand, Johannesburg. An immense note of gratitude and indebtedness is extended to Mrs M.C. Keeton and to the Board of Trustees. The graphic enhancement used for Figure 2 was done by DLB using SAOIMAGE and the CIBA process. ISO is an ESA project with instruments funded by ESA member states (especially the PI countries: France, Germany, the Netherlands and the United Kingdom) and with participation of ISAS and NASA. It is also a great pleasure to thank Steven Lambert for his assistance. We dedicate this paper to Professor J.M. Greenberg, on the occassion of his 75th birthday.

References

[1] Aaronson, M., Mould, J.: 1983, *ApJ.* **265**, 1

[2] Allen, R.J., Lequeux, J.: 1993, *ApJ.* **410**, L15

[3] Allen, R.J.: 1996, in *New Extragalactic Perspectives in the New South Africa* (eds. Block, D.L. & Greenberg, J.M.) Kluwer Academic Press, Dordrecht; p50

[4] Andreani, P., Franceschini,A.: 1992, *A & A.* **260**, 89

[5] Andriesse, C.D.: 1977, 'Radiating cosmic dust' in *Vistas in Astronomy* **21**, 107

[6] Antonucci, R.R.: 1993, *Ann. Rev. Astron. Astrophys*, **31**, 473.

[7] Begeman, K.: 1987, *HI Rotation Curves of Spiral Galaxies*, PhD Thesis, Univ Groningen

[8] Bernard, J.P., Boulanger, F., Puget, J.L.: 1993, *A & A.* **277**, 609

[9] Bertin, G., Lin, C.C., Lowe, S.A., Thurstans, R.P.: 1989, *ApJ.* **338**, 78

[10] Bertin, G., Lin, C.C., Lowe, S.A., Thurstans, R.P.: 1989, *ApJ.* **338**, 104

[11] Bertin, G.: 1996, in *New Extragalactic Perspectives in the New South Africa* (eds. Block, D.L. & Greenberg, J.M.) Kluwer Academic Press, Dordrecht; p227

[12] Blitz, L., Thaddeus, P.: 1980, *ApJ.* **241**, 646

[13] Block, D.L.: 1990, *Nature.* **347**, 452

[14] Block, D.L., Wainscoat, R.J.: 1991, *Nature.* **353**, 48

[15] Block, D.L., Bertin, G., Stockton, A., Grosbøl, P., Moorwood, A.F.M., Peletier, R.F.: 1994, *A & A* **288**, 365 (Paper I)

[16] Block, D.L., Witt, A.N., Grosbøl, P., Stockton, A., Moneti, A.: 1994, *A & A* **288**, 383 (Paper II)

[17] Block, D.L., Witt, A.N. & Grosbøl, P.: 1995, in *The Opacity of Spiral Disks* (ed J.I. Davies and D. Burstein, Kluwer) p. 227

[18] Block, D.L., Elmegreen, B.G., Wainscoat, R.J.: 1996, *Nature* **381**, 674

[19] Block, D.L.: 1996, in *New Extragalactic Perspectives in the New South Africa* (eds. Block, D.L. & Greenberg, J.M.) Kluwer Academic Press, Dordrecht; p1

[20] Bosma, A.: 1981, *Astr. J.* **86**, 1825

[21] Boulade, O. et al.: 1996, *A & A*, **315**, L85

[22] Braine, J., Combes, F.: 1992, *A & A. Suppl.* **264**, 433

[23] Byrd, G., Salo, H. 1995, *Astrophys.Lett.Comm.* **36**, Nos. 1-6, 193

[24] Carico, D.P., Keene, J., Soifer, B.T., Neugebauer, G.: 1992, *PASP.* **104**, 1086

[25] Cesarsky, C.J. et al.: 1996, A & A. **315**, L32 1193

[26] Chini, R., Krügel, E.: 1993, *A & A.* **279**, 385

[27] Clements, D.L., Andreani, P., Chase, S.T.: 1993, *MNRAS.* **261**, 299

[28] Désert, F.X., Boulanger, F., Puget, J.L: 1990, A & A, **237**, 215

[29] Draine, B.T. & Anderson, N.: 1985, *ApJ*, **292**, 494

[30] Draine, B.T. & Lee, H.M.: 1984, *ApJ.* **285**, 89

[31] Duley, W.W.: 1996, in *New Extragalactic Perspectives in the New South Africa* (eds. Block, D.L. & Greenberg, J.M.) Kluwer Academic Press, Dordrecht; p29

[32] Devereux, N.A., Young, J.S.: 1990, *ApJ.* **359**, 42

[33] Devereux, N.A., Young, J.S.: 1992, *AJ.* **103**, 1536

[34] Eales, S.A., Wynn-Williams, C.G., Duncan, W.D.: 1989, *ApJ.* **339**, 859

[35] Elmegreen, D.M., & Elmegreen, B.G.: 1984, *Astrophys. J. Suppl*, **54**, 127

[36] Elmegreen, B.G. & Elmegreen, D.M.: 1986, *ApJ.* **311**, 554

[37] Elmegreen, B.G., Elmegreen, D.M., & Montenegro, L.: 1992, *ApJ. Supp.* **79**, 37

[38] Elmegreen, B.G.: 1994, *ApJ.* **433**, 39

[39] Garcia-Burillo, S., Guelin, M., Cernicharo, J.: 1993, *A & A.* **274**, 123

[40] Gérin, M., Casoli, F., Combes, F.: 1991, *A & A.* **251**, 32

[41] Gordon, M.A.: 1995, *A & A* **301**, 853

[42] Greenberg, J.M.: in *Stars and Stellar Systems*, **VII**, (ed. B.M. Middlehurst and L.H. Aller, Univ. Chicago Press, Chicago), p221

[43] Greenberg, J.M.: 1970, *Interstellar grains and spiral structure* in *Interstellar Gas Dynamics* (ed. H.J. Habing, Reidel, Dordrecht), 305

[44] Greenberg, J.M.: 1973, in *Molecules in the Galactic Environment* (ed. Gordon, M.A. and Snyder, L.E.) Wiley, p94

[45] Greenberg, J.M.: 1978, in *Cosmic Dust* (ed. J.A.M. McDonnell), Wiley InterScience, p279

[46] Greenberg, J.M. & Li, A.: 1996, in *New Extragalactic Perspectives in the New South Africa* (eds. Block, D.L. & Greenberg, J.M.) Kluwer Academic Press, Dordrecht; p118

[47] Grosbøl, P. & Patsis, P.: 1996, in *New Extragalactic Perspectives in the New South Africa* (eds. Block, D.L. & Greenberg, J.M.) Kluwer Academic Press, Dordrecht; p251

[48] Guillois, O., Nenner, I., Papoular, R., Reynaud, C.: 1996, *ApJ.* **464**, 810

[49] Heckman, T.M.: 1980, A & A. **87**, 152

[50] Hildebrand, R.H.: 1983, *QJRAS.* **24**, 267

[51] Hobson, M.P., Scheuer, P.A.G.: 1993, *MNRAS.* **264**, 145

[52] Hobson, M.P., Padman, R.: 1993, *MNRAS.* **264**, 161

[53] Hobson, M.P., Padman, R.: 1994, *MNRAS.* **266**, 752

[54] Hodge, P.W.: 1980, *AJ.* **85**, 376

[55] Johnson, H.M. & Hanna, M.M.: 1972, *ApJ.* **174**, L71

[56] Kessler, M.F. et al.: 1996, *A & A.* **315**, L27

[57] Kim, S.-H., Martin, P.G., Hendry, P.D.: 1994, *ApJ.* **422**, 164

[58] Kormendy, J.: 1977, in *The Evolution of Galaxies and Stellar Populations* (ed. B.M. Tinsley & R.B. Larson, Yale Univ: New Haven), 131

[59] Kormendy, J.: 1993, in *Galactic Bulges* (ed. H.J. Habing & H. de Jongh) (IAU Symp. No. 153) Dordrecht: Kluwer.

[60] Kormendy, J.: 1982, *Observations of Galaxy Structure and Dynamics*, 12th Advanced Course: SAAS-FEE 1982, Geneva Observatory, 113

[61] Kwan, J., Xie, S.: 1992, *ApJ.* **398**, 105

[62] Léger, A. & Puget, J.L.: 1984, *A & A.* **137**, L5

[63] Lehtinen, K. & Mattila, K. 1996, *A & A.* **309**, 570

[64] Lequeux, J., Allen, R.J., Guilloteau, S.: 1993, *A & A.* **280**, L23

[65] Lequeux, J.: 1994, *A & A.* **287**, 368

[66] Lynds, B.T.: 1974, *ApJS.* **28**, 391

[67] Milliard, B., Marcelin, M.: 1981, *A & A.* **95**, 59

[68] Marcelin, M., Comte, G., Courtes, G., Georgelin, Y.P., Milliard, B.: 1980, *PASP.* **92**, 38

[69] Maddalena, R., Thaddeus, P.: 1985, *ApJ.* **294**, 231

[70] Mathis, J.S.: 1996, *ApJ.* **472**, 643.

[71] McElroy, D.B.: 1983, *ApJ.* **270**, 485

[72] Pajot, F., Boissé, P., Gisbert, A., Lamarre, J.M., Puget, J.L., Serra, G.: 1986, *A & A.* **157**, 393

[73] Pfenniger, D., Combes, F.: 1994, *A & A.* **285**, 94

[74] Rand, R.J., Kulkarni, S.R.: 1990, *ApJ.* **349**, L43

[75] Rand, R.J.: 1993, *ApJ.* **404**, 593

[76] Rich, R.M., Mighell, K.J., Neill, J.D. & Freedman, W.: 1996, in *New Extragalactic Perspectives in the New South Africa* (eds. Block, D.L. & Greenberg, J.M.) Kluwer Academic Press, Dordrecht; p325

[77] Rix, H-W., & Rieke, M.J.: 1993, *Astrophys. J.*, **418**, 123

[78] Rix, H-W & Zaritsky, D.: 1994, in *Infrared Astronomy with Arrays: The Next Generation* (ed. I.S. McLean; Kluwer), 151

[79] Roche, P.F., Aitken, D.K.: 1985, *MNRAS.* **213**, 789

[80] Rodriguez-Espinosa, J.M., Perez-Garcia., Lemke, D. et al.: 1996, *A & A*, **315**, L129

[81] Rots, A.H., Crane, P.C., Bosma, A., Athanassoula, E., & van der Hulst, J.M.: 1990, *Astron. J.* **100**, 387

[82] Sage, L.J.: 1993, *A & A.* **272**, 123

[83] Sage, L.J., Wrobel, J.M.: 1989, *ApJ*, **344**, 204

[84] Sandage, A.: 1961, *Hubble Atlas of Galaxies.* Washington DC: Carnegie Institution

[85] Sandage, A., Tammann, G.A.: 1981, *A Revised Shapley-Ames Catalogue of Bright Galaxies* Washington DC: Carnegie Institution

[86] Sandage, A., Bedke, J.: 1994, *The Carnegie Atlas of Galaxies* Washington DC: Carnegie Institution

[87] Sanders, D.B., Scoville, N.Z., Soifer, B.T.: 1991, *ApJ.* **370**, 158

[88] Sauvage, M., Thuan, T.X.: 1994, *ApJ.* **429**, 153

[89] Sauvage, M. et al.: 1996, A & A. **315**, L89

[90] Sellgren, K., Werner, M.W., Dinerstein, H.L.: 1983, *ApJ.* **271** L13

[91] Sellgren, K.: 1996, in *New Extragalactic Perspectives in the New South Africa* (eds. Block, D.L. & Greenberg, J.M.) Kluwer Academic Press, Dordrecht; p151

[92] Smith, J.: 1982, *ApJ.* **261**, 463

[93] Smith, B.J., Harvey, P.M., Colome, C., Zhang, C.Y., DiFrancesco, J., Pogge, R.W.: 1994, *ApJ.* **425**, 91

[94] Smith, B.J.: 1996, in *New Extragalactic Perspectives in the New South Africa* (eds. Block, D.L. & Greenberg, J.M.) Kluwer Academic Press, Dordrecht; p170

[95] Stark, A.A., Davidson, J.A., Harper, D.A., Pernic, R., Loewenstein, R., Platt, S., Engargiola, G., Casey, S.: 1989, *ApJ.* **337**, 650

[96] Thornley, M.D.: 1996, *ApJ.* **469**, L45

[97] Thornley, M.D.: 1996, in *New Extragalactic Perspectives in the New South Africa* (eds. Block, D.L. & Greenberg, J.M.) Kluwer Academic Press, Dordrecht; p566

[98] Valentijn, E.A., van der Werf, P.P., de Graauw, T. et al.: 1996, *A & A*, 315, L145

[99] van der Hulst, J.M., Kennicutt, R.C., Crane, P.C., Rots, A.H.: 1988, A & A. **195**, 38

[100] Williams, J.P., de Geus, E.J., Blitz, L.: 1994, *ApJ.* **428**, 693

[101] Witt, A.N., Thronson, H.A., Capuano, J.M.: 1992, *ApJ.* **393**, 611

[102] Witt, A.N., Lindell, R.S., Block, D.L., Evans, R.: 1994, *ApJ.* **427**, 227

[103] Woltjer, L.: 1965, in Stars and Stellar Systems, **5** *Galactic Structure* (ed. A. Blaauw & M. Schmidt, Univ Chicago Press) 531

[104] Woodward, P.R.: 1976, *ApJ.* **207**, 484

[105] Wray, J.D.: 1988, *Colour Atlas of Galaxies* Cambridge University Press.

[106] Young, J.S. & Scoville, N.: 1982, *Astrophys.J.* **260**, L41

[107] Zaritsky, D., Rix, H-W., Rieke, M.J.: 1993, *Nature* **364**, 313